Applied Nanoscience (2020) 10:5489–5497
https://doi.org/10.1007/s13204-020-01431-w

ORIGINAL ARTICLE

Thermal analysis in unsteady radiative Maxwell nanofluid flow subject to heat source/sink

Awais Ahmed[1] · Masood Khan[1] · Abdul Hafeez[1] · Jawad Ahmed[1,2]

Received: 5 March 2020 / Accepted: 23 April 2020 / Published online: 25 May 2020

Abstract

Currently, various researchers achieved theoretical and experimental works to scrutinize the influence of nanofluid in diverse forms of heat exchangers. In any engineering applications heat exchangers are critical components. Nanofluids are colloidal assortment of non-metallic or metallic particles suspended in base liquid. This study communicates a critical analysis of heat transport application of nanofluid. We established a model for unsteady flow of Maxwell nanofluid with the aspect of thermal radiation due to stretched cylinder. Moreover, heat source/sink is considered. Appropriate conversions yield the ordinary differential equations (ODEs) and then solved via homotopic methodology. Graphical outcomes of the velocity, temperature and concentration fields for influential parameters are plotted and discussed physically. The achieved outcomes specify that the temperature and concentration distribution increases for the higher unsteadiness parameter, curvature parameter and Maxwell parameter. Moreover, both thermophoresis and Brownian motion parameters enhances the thermal energy transport in flow.

Keywords Maxwell fluid model · Unsteady flow · Nanofluid · Thermal radiation · Heat source/sink

Introduction

The subject of the heat transfer analysis attract the researchers now a days due its importance in the many engineering areas specially the heat transport in the fluid flow. Such as production of plastic and polymers needs the higher rate of heat transport for the better quality of the product. To replace the working liquids with nanoparticles as a innovative approach to enhance the heat transport phenomena in liquid. Nanofluid is a colloidal fusion where the possession of both nanomaterials and base liquids provide the change in the transport and thermal aspects of base liquids. In recent, diverse sorts of nanoparticles, for the instance, metallic and ceramic nanoparticles, have been utilized for formation of nanofluids. The notion of nanofluids concerning heat transport enhancement through dense particles of nano-meter was reported by Choi (1995). Hsiao (2016) analyzed the mixed convective stagnation point flow of nanofluid with the slip boundary condition on the stretching sheet. Magnetohydrodynamics flow of micropolar nanofluid over stretching sheet under the impact of viscous dissipation was reported by Hsiao (2017). This study revealed that both magnetic parameter and Eckert number enhance the temperature field. By utilizing FEM scheme, Haq and Aman (2019) investigated the performance of CuO nanoparticles with inner heated obstacle, in partially heated trapezoidal cavity. Xu et al. (2019) studied the phenomena of thermal radiation, heat convection/conduction and phase change heat transport to nanofluid. The properties of radiation and chemical reaction in Maxwell nanofluid were addressed by Hayat et al. (2019). Impacts of activation energy and chemical reaction in peristaltic blood flow with nanoparticles was explored by Ellahi et al. (2019). They noted that the gold particles condenses large particles to transport important drugs powerfully to the effected portion of the organ. Additionally, relevant works dealing with nanofluid were reported in see Refs. Irfan et al. (2019), Mahanthesh and Joseph (2019), Khan et al. (2019), Turkyilmazoglu (2019a), Turkyilmazoglu (2019b) and Turkyilmazoglu (2020).

Recently, the study of non-linear fluids have noteworthy consideration due to their practical applications in engineering and trade. For instance, piping, extrusion methodology in metallurgy, in large scale cooling/heating structures, and

✉ Abdul Hafeez
ahafeez@math.qau.edu.pk

[1] Department of Mathematics, Quaid-i-Azam University, Islamabad 44000, Pakistan

[2] Department of Basic Sciences, University of Engineering and Technology, Taxila 47050, Pakistan

oil recovery etc includes the flow of non-linear liquids. To increase the efficiency in thermal extrusion manufacturing Hsiao (2017a), Hsiao (2017b) studied the flow of non-Newtonian nanofluid with impact of thermal radiation, magnetic field and viscous dissipation. One important aspect of these fluids is their advanced apparent viscosity. Additionally, various researchers have reported their investigations for the flow of non-linear fluids with diverse aspects (see Refs Malik and Khan 2018; Bai et al. 2019; Moshkin et al. 2019; Khan and Nadeem 2019; Hamid et al. 2018). The considered Maxwell fluid model is the special type of non-Newtonian fluid in which the characteristics of both elastic and viscous forces are described. This model is good for viscoelastic fluids because it can described the stress relaxation phenomenon accurately in these types of fluid. Ahmed et al. (2019) analyzed thin film flow Maxwell fluid with heat transport in the presence of non-linear radiation. The convective phenomena on Maxwell fluid utilizing Brownian and thermophrotic forces for nanofluid was studied by Khan et al. (2019).

In view of the above studies, we noted that no study has been made to report the unsteady flow of Maxwell nanofluid towards stretched cylinder. Thus, the present analysis is reported to investigate the flow and heat transport of Maxwell nanofluid with impact of heat source/sink and thermal radiation. Additionally, the Brownian and thermophoretic forces are taken in account to study the convective heat transport enhancement. The well known homotopic approach (Turkyilmazoglu 2011, 2012, 2018) is employed for solutions of the governing problem. The results are presented graphically and validated through tabular data.

Mathematical formulation

Consider 2D unsteady flow of Maxwell nanofluid induced by stretching cylinder of radius R_1. The cylinder is stretched with velocity $u(t,z)=\frac{az}{1-\gamma t}$ along z–direction, where $a=\frac{U_0}{L}$ is the stretching rate, γ the positive constant with property $\gamma t \leq 1$. Let the cylindrical polar coordinates (z, r) are taken to be in such approach that $z-axis$ runs along the axis of the cylinder and $r-axis$ is restrained perpendicular to it as exposed in blow (Fig. 1). Additionally, heat sink/source aspects are considered. Under above consideration the governing boundary layer equations (Moshkin et al. 2019; Khan et al. 2019) for Maxwell nanofluid model are specified as follows.

$$\frac{\partial(ru)}{\partial z}+\frac{\partial(rw)}{\partial r}=0, \tag{1}$$

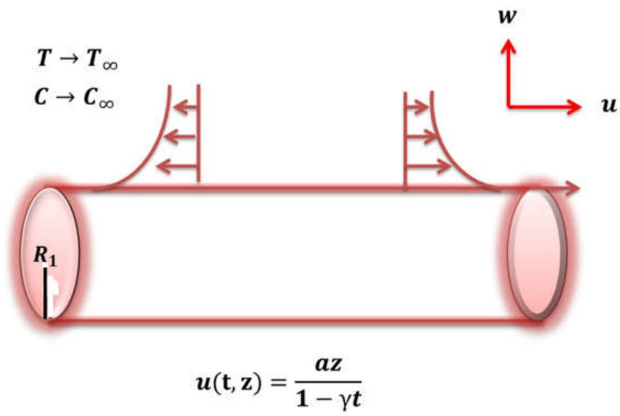

Fig. 1 Physical sketch of the problem

$$\begin{aligned}\frac{\partial u}{\partial t}+u\frac{\partial u}{\partial z}+w\frac{\partial u}{\partial r}&=\nu\left[\frac{\partial^2 u}{\partial r^2}+\frac{1}{r}\frac{\partial u}{\partial r}\right]\\&-\lambda_1\left[\frac{\partial^2 u}{\partial t^2}+2u\frac{\partial^2 u}{\partial t\partial z}+2w\frac{\partial^2 u}{\partial r\partial t}\right.\\&\left.+2uw\frac{\partial^2 u}{\partial r\partial z}+w^2\frac{\partial^2 u}{\partial r^2}+u^2\frac{\partial^2 u}{\partial z^2}\right],\end{aligned} \tag{2}$$

$$\begin{aligned}\frac{\partial T}{\partial t}+u\frac{\partial T}{\partial z}+w\frac{\partial T}{\partial r}&=\alpha_1\left[\frac{\partial^2 T}{\partial r^2}+\frac{1}{r}\frac{\partial T}{\partial r}\right]\\&-\frac{1}{(\rho c)_f}\left[\frac{1}{r}\frac{\partial}{\partial r}(rq_r)\right]\\&+\tau\left[D_B\frac{\partial C}{\partial r}\frac{\partial T}{\partial r}+\frac{D_T}{T_\infty}\left(\frac{\partial T}{\partial r}\right)^2\right]+Q_\circ\left(\frac{T-T_\infty}{(\rho c)_f}\right),\end{aligned} \tag{3}$$

$$\begin{aligned}\frac{\partial C}{\partial t}+u\frac{\partial C}{\partial z}+w\frac{\partial C}{\partial r}&=D_B\frac{1}{r}\frac{\partial}{\partial r}\left[\left(r\frac{\partial C}{\partial r}\right)\right]\\&+\frac{D_T}{T_\infty}\frac{1}{r}\frac{\partial}{\partial r}\left[\left(r\frac{\partial T}{\partial r}\right)\right],\end{aligned} \tag{4}$$

with boundary conditions

$$\begin{aligned}&u(t,z,r)=u(t,z)=\frac{az}{1-\gamma t},\ w(t,z,r)=0,\\&T=T_w,\ C=C_w \text{ at } r=R_1,\end{aligned} \tag{5}$$

$$u\to 0,\ T\to T_\infty,\ C\to C_\infty \text{ as } r\to\infty. \tag{6}$$

Here (u, w) are the velocity components in the z– and r–directions, respectively, ν the kinematic viscosity, λ_1 the relaxation time, α_1 the thermal diffusivity, (T, C) the temperature and concentration of fluid, τ the heat capacity ratio of nanoparticles to base fluid and Q_0 the source/sink, T_w and C_w the wall temperature and concentration, respectively, T_∞ and C_∞ the ambient temperature and concentration of fluid,

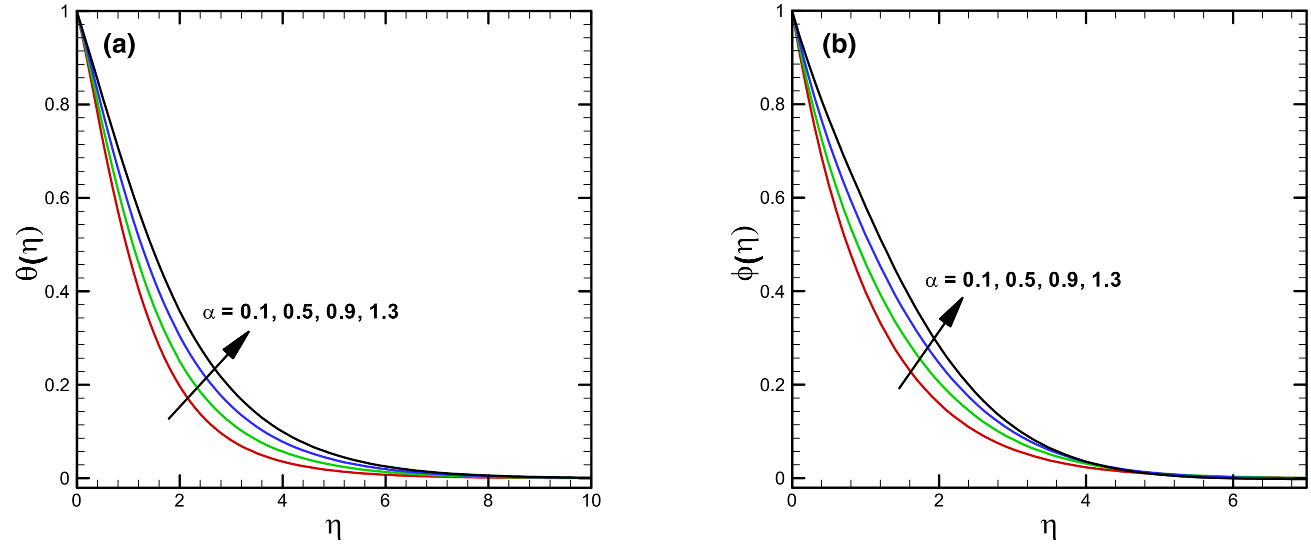

Fig. 2 Impact of curvature parameter α on $\theta(\eta)$ and $\phi(\eta)$

respectively, (D_B, D_T) the Brownian and thermophoresis diffusion coefficients, respectively. q_r the radiative heat flux which defined as $q_r = \frac{-16\sigma^*}{3k*} T_\infty^3 \frac{\partial T}{\partial r}$ where $(\sigma^*, k*)$ the Stefan -Boltzmann constant and mean absorption coefficient, respectively.

Introducing the following conversions

$$u = \frac{az}{1-\gamma t} f'(\eta),\ w = -\frac{R_1}{r}\sqrt{\frac{a\nu}{(1-\gamma t)}} f(\eta),\ \theta(\eta) = \frac{T - T_\infty}{T_w - T_\infty},$$
$$\phi(\eta) = \frac{C - C_\infty}{C_w - C_\infty},\ \eta = \sqrt{\frac{a}{\nu(1-\gamma t)}}\left(\frac{r^2 - R_1^2}{2R_1}\right). \quad (7)$$

Above conversions yield the following ODEs of Maxwell nanofluid flow with energy transport:

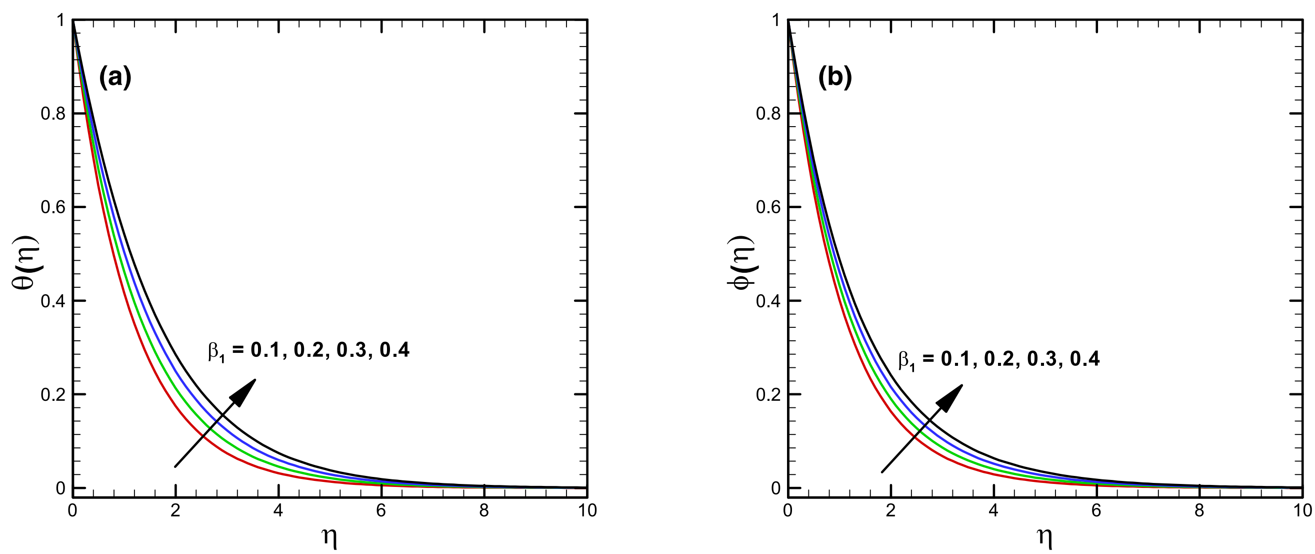

Fig. 3 Impact of Maxwell parameter β_1 on $\theta(\eta)$ and $\phi(\eta)$

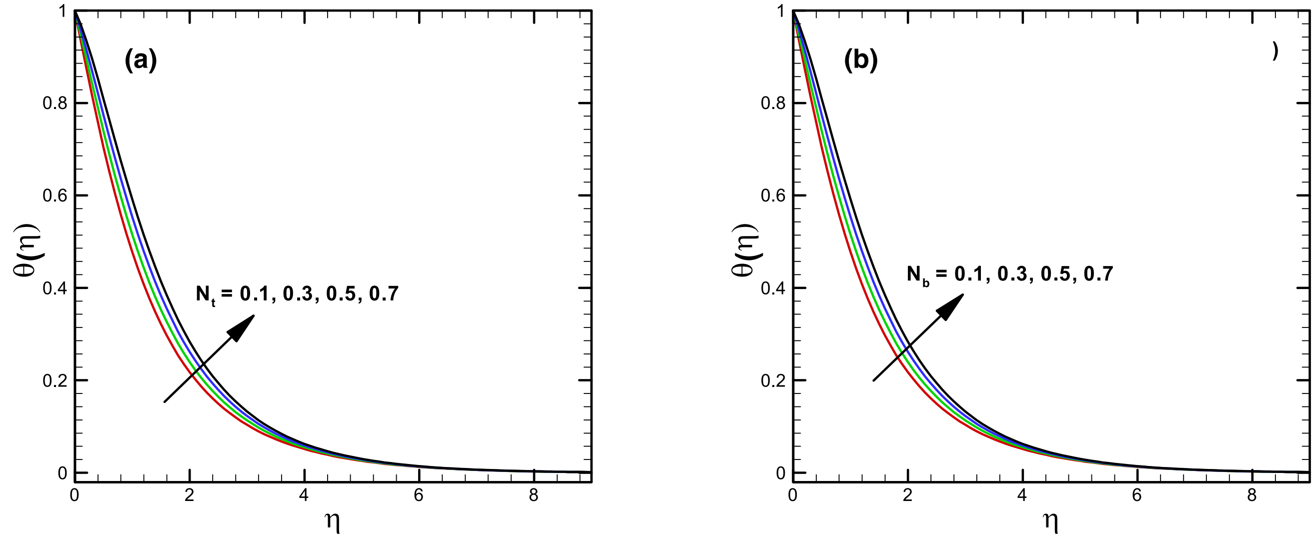

Fig. 4 Impact of thermophoresis N_t and Brownian motion parameters N_b on $\theta(\eta)$

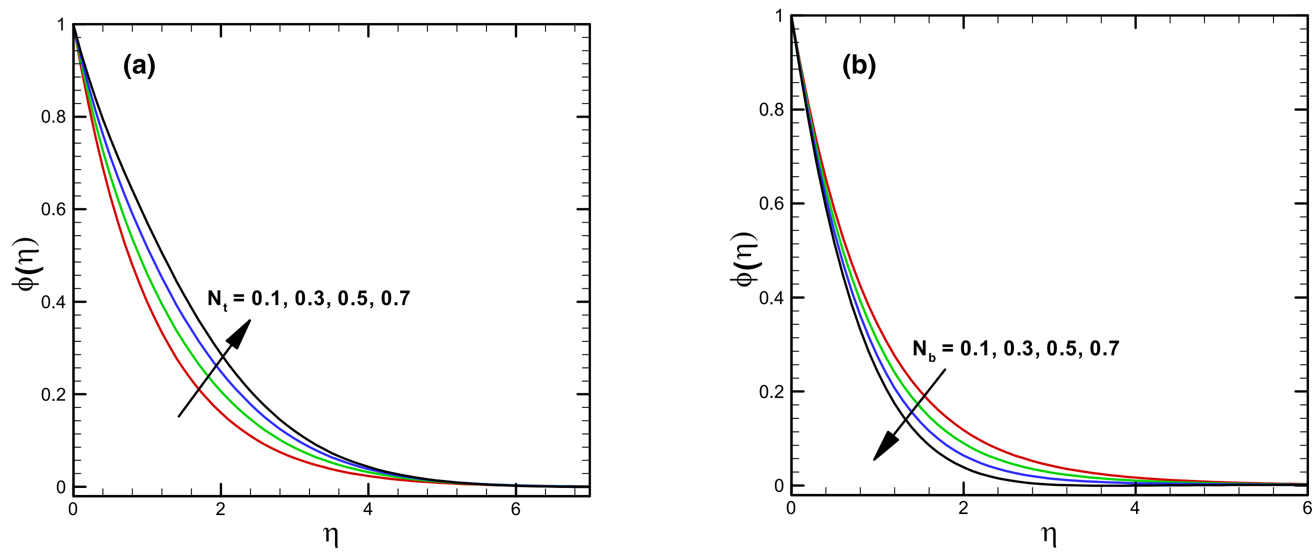

Fig. 5 Impact of thermophoresis N_t and Brownian motion parameter N_b on $\phi(\eta)$

$$
\begin{aligned}
&(1+2\alpha\eta)f''' + 2\alpha ff'' - \frac{S}{2}\eta f'' - Sf' \\
&\quad - f'^2 + ff'' - \frac{7}{4}\beta_1 S^2 \eta f'' \\
&\quad - \frac{\beta_1}{4}\eta^2 S^2 f''' - 2\beta_1 S^2 f' - 2S\beta_1 f'^2 \\
&\quad - \beta_1 \eta S f' f'' + 3S\beta_1 ff'' \\
&\quad + S\beta_1 \eta ff''' + 2\beta_1 ff' f'' \\
&\quad - \frac{\alpha\beta_1}{1+2\alpha\eta} f^2 f'' - \beta_1 f^2 f''' = 0,
\end{aligned} \tag{8}
$$

$$
\begin{aligned}
&(1+\frac{4}{3}R_d)(1+2\alpha\eta)\theta'' + 2\alpha\theta' + \Pr f\theta' - \Pr\frac{S}{2}\eta\theta' \\
&\quad + (1+2\alpha\eta)\Pr N_b\theta'\phi' + (1+2\alpha\eta)\Pr N_t\theta'^2 + \Pr\delta\theta = 0,
\end{aligned} \tag{9}
$$

$$
\begin{aligned}
&(1+2\alpha\eta)\phi'' + 2\alpha\phi' + Le\Pr f\phi' - Le\Pr\frac{S}{2}\eta\phi' \\
&\quad + (1+2\alpha\eta)\left(\frac{N_t}{N_b}\right)\theta'' + 2\alpha\left(\frac{N_t}{N_b}\right)\theta' = 0,
\end{aligned} \tag{10}
$$

with boundary conditions

$$
f(0) = 0,\ f'(0) = 1,\ \theta(0) = 1,\ \phi(0) = 1, \tag{11}
$$

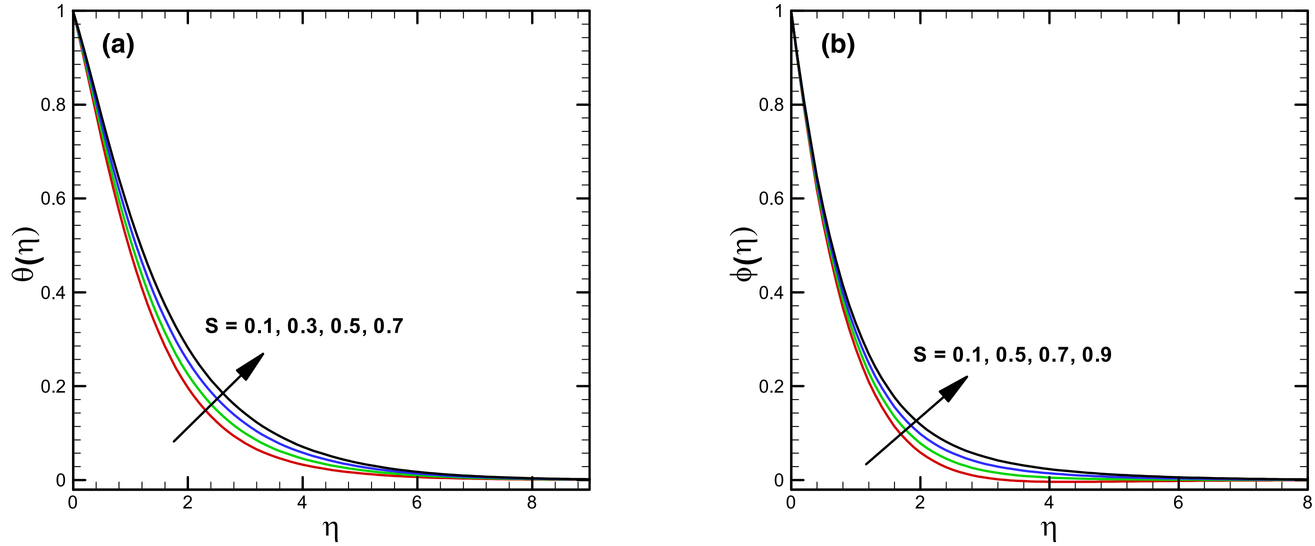

Fig. 6 Impact of unsteadiness parameter S on $\theta(\eta)$ and $\phi(\eta)$

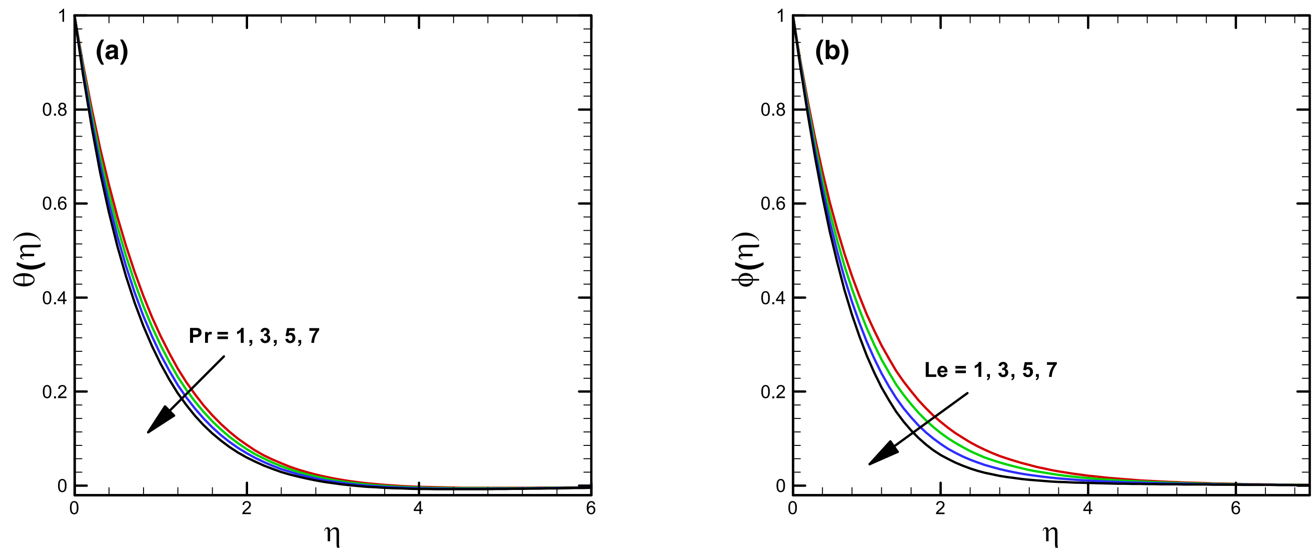

Fig. 7 Impact of Prandtl number Pr and Lewis number Le on $\theta(\eta)$ and $\phi(\eta)$, respectively

$$f'(\infty) = 0,\ \theta(\infty) = 0,\ \phi(\infty) = 0. \tag{12}$$

Where $S\left(=\frac{\gamma}{a}\right)$ is the unsteadiness parameter, $\alpha\left(=\frac{1}{R_1}\sqrt{\frac{\nu(1-\gamma t)}{a}}\right)$ the curvature parameter, $\beta_1\left(=\frac{\lambda_1 a}{1-\gamma t}\right)$ the Maxwell parameter, $\Pr\left(=\frac{\nu}{\alpha_1}\right)$ the Prandtl number, $N_b\left(=\frac{\tau D_B(C_w-C_\infty)}{\nu}\right)$ the Brownian motion parameter, $N_t\left(=\frac{\tau D_T(T_w-T_\infty)}{\nu T_\infty}\right)$ the thermophoresis parameter, $Le\left(=\frac{\alpha_1}{D_B}\right)$ the Lewis number, $R_d\left(=\frac{4\sigma^* T_\infty^3}{kk^*}\right)$ radiation parameter and $\delta\left(=\frac{Q_0(1-\gamma t)}{a(\rho c)_f}\right)$ the heat source/sink parameter.

Physical quantities

Expressions for the local Nusselt (Nu_z) and local Sherwood (Sh_z) numbers are

$$Nu_z = \frac{zq_s}{k(T_w - T_\infty)},\quad Sh_z = \frac{zj_s}{D_B(C_w - C_\infty)}, \tag{13}$$

where q_s and j_s are the heat and mass fluxes, respectively,

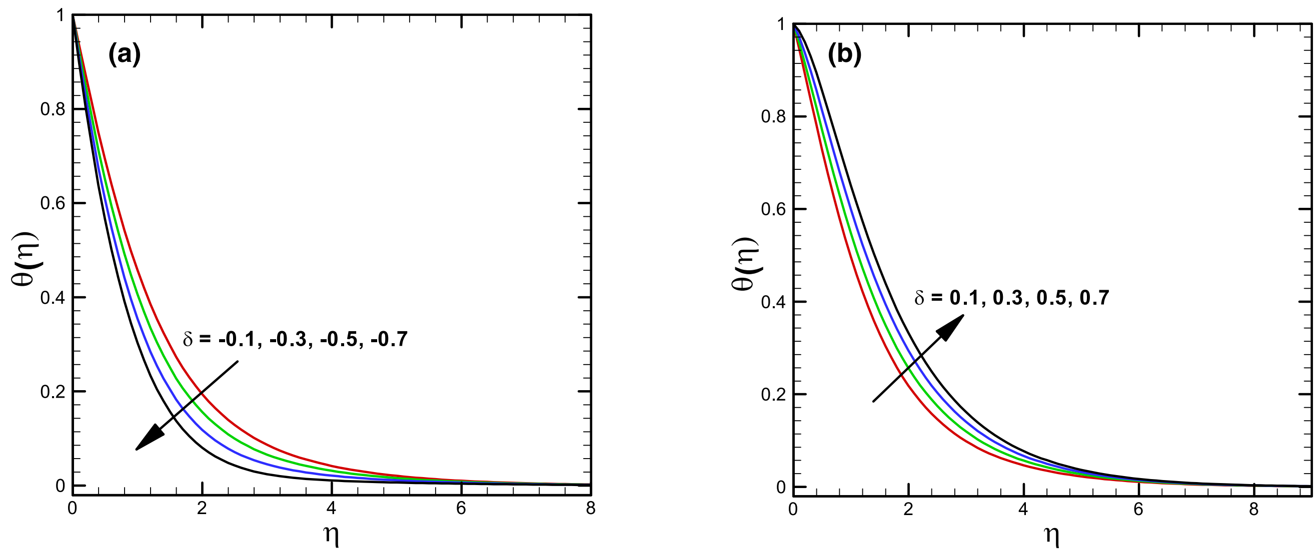

Fig. 8 Impact of heat sink $\delta < 0$ and heat source $\delta > 0$ on $\theta(\eta)$

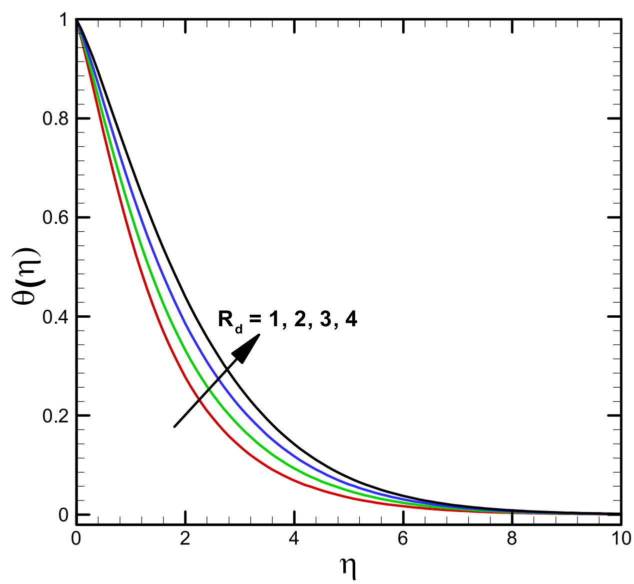

Fig. 9 Impact of radiation parameter R_d on $\theta(\eta)$

$$q_s = -k\left(\frac{\partial T}{\partial r}\right)_{r=R_1} - \frac{4\sigma^* T_\infty^3}{3k^*}\left(\frac{\partial T}{\partial r}\right)_{r=R_1}, \quad j_s = -D_B\left(\frac{\partial C}{\partial r}\right)_{r=R_1}, \tag{14}$$

in dimensionless forms these are given by

$$Nu_z \mathrm{Re}_z^{-\frac{1}{2}} = -\left(1 + \frac{4R_d}{3}\right)\theta'(0), \quad Sh_z \mathrm{Re}_z^{-\frac{1}{2}} = -\phi'(0), \tag{15}$$

where $\mathrm{Re}_z = \frac{u(t,z)z}{\nu}$ signifies the Reynolds number.

Solution scheme

To achieve the series solutions of Eqs. (8)–(10) along the boundary conditions given in Eqs. (11, 12) the well known homotopy analysis method for the highly non-linear ordinary differential system has been utilized. The following

Table 1 A comparison of $-f''(0)$ for β_1 when $\alpha = S = 0$

$-f''(0)$					
β_1	Ref. Abel et al. (2012)	Ref. Megahed (2013)	Ref. Waqas et al. (2017)	Ref. Irfan et al. (2019)	Present
0.0	1.000000	0.999978	1.000000	1.0000000	1.000000
0.2	1.051948	1.051945	1.051889	1.0518890	1.051890
0.4	1.101850	1.101848	1.101903	1.1019035	1.101903
0.6	1.150163	1.150160	1.150137	1.1501374	1.150137
0.8	1.196692	1.196690	1.196711	1.1967114	1.196711
1.0					1.241747
1.2	1.285257	1.285253	1.285363	1.2853630	1.285364

Table 2 A comparison of $f''(0)$ for S when $\alpha = \beta_1 = 0$

$f''(0)$				
S	Ref. Sharidan et al. (2006)	Ref. Chamkha et al. (2010)	Ref. Irfan et al. (2017)	Present
0.8	−1.261042	−1.261512	−1.261044	−1.261043
1.0				−1.320522
1.2	−1.377722	−1.378052	−1.377728	−1.377722
1.3				−1.405538
2.0	−1.587362		−1.587371	−1.587372

Table 3 A comparison of $-\theta'(0)$ for Pr when $\alpha = S = \beta_1 = N_t = R_d = \delta = 0$, and $N_b \to 0$

$-\theta'(0)$				
Pr	Ref. Khan and Pop (2010)	Ref. Wang (1989)	Ref. Gorla and Sidawi (1994)	Present
0.7	0.4539	0.4539	0.4539	0.453919
1.0				0.581974
1.5				0.760289
2.0	0.9113	0.9114	0.9114	0.911156

initial estimates (f_0, θ_0, ϕ_0) and linear operators $(\pounds_f, \pounds_\theta, \pounds_\phi)$ are selected for the governing problem as

$$f_0(\eta) = 1 - e^{-\eta},\ \theta_0(\eta) = e^{-\eta},\ \phi_0(\eta) = e^{-\eta}, \tag{16}$$

$$\pounds_f[f(\eta)] = f''' - f', \pounds_\theta[\theta(\eta)] = \theta'' - \theta, \pounds_\phi[\phi(\eta)] = \phi'' - \phi. \tag{17}$$

Results and discussion

This section discusses the aspects of influential parameters on the velocity, temperature and concentration fields via homotopic scheme. The outcomes for scheming parameters are graphed and discussed in detail with physical arguments. The value of physical parameters are taken to be fixed as $S = \beta_1 = \alpha = R_d = 0.5$, $\delta = 0.2$, $N_t = N_b = 0.4$ and $Le = \text{Pr} = 7$. Figure 2 illustrate the effect of curvature parameter α on nanoliquid temperature and concentration fields. We observed that the temperature, and concentration fields of Maxwell nanoliquid are increasing function of α. Physically, rise in the curvature parameter α declines the radius of cylinder due to which the interaction region of the cylinder with the liquid is diminished. Hence, fluid

Table 4 Numerical values of Nusselt number and Sherwood number for various values of N_t, N_b, R_d and with fixed $S = \alpha = \beta_1 = 0.5$ and $\delta = 0.2$

N_t	N_b	R_d	Pr	Le	$-(1+\frac{4}{3}R_d)\theta'(0)$ (bvp4c)	$-\phi(0)$ (bvp4c)
0.1	0.1	0.1	6.5	1	1.034140	2.098520
0.2					0.802809	2.287901
0.3					0.621628	2.281950
0.4					0.478501	2.290000
0.1	0.1	0.1	6.5	1	1.034140	2.098520
	0.2				0.675387	2.252790
	0.3				0.418133	2.277501
	0.4				0.241032	2.275660
0.1	0.1	0.1	6.5	1	1.034140	
		0.2			1.038640	
		0.3			1.034230	
		0.4			1.022940	
0.1	0.1	0.1	01		1.034140	
			02		0.990373	
			03		0.908140	
			04		0.808253	
0.1	0.1	0.1	6.5	01		2.098052
				02		3.114500
				03		3.839540
				04		4.430770

influenced in stretching cylinder is less. Furthermore, we noted that the higher values of α enhance both the temperature and its allied thermal thickness of boundary layer. The impact of α on temperature field is more prominent than the concentration field. The temperature and concentration fields for Maxwell parameter are portrayed in Fig. 3. From these interpretation, it is observed that the intensification in β_1 enhances both the temperature and concentration distribution in Maxwell liquid. As β_1 is the ratio of relaxation time to observation time and rise in β_1 means there is higher the relaxation time in the fluid. Due to which the fluid becomes solid like and consequently, the conduction of thermal and solutal energy increases in the fluid motion. Figures 4 and 5 are represented to envision the impact of thermophoresis N_t and Brownian motion N_b parameters on nanoliquid temperature and concentration fields. Here, we reported that a rise in the value of N_t enhances both the temperature and concentration fields. Physically, higher value of N_t enhances the temperature difference between wall and free stream. Hence, the heat transfer rate is enhanced which enhances the temperature field. Furthermore, rise in Brownian motion parameter N_b causes the enhance of temperature field. Because for higher value of N_b the collision of nanoparticles boost up which intensify the temperature field. On the other hand, concentration field declines with higher values of N_b. Physically, for higher values of N_b the particles collision provides the disturbance for mass transfer and thus, as a result the declines in concentration field is noted. To picture the impact of unsteadiness parameter S on nanoliquid temperature and concentration of Maxwell fluid Fig. 6 are delineated. We observed that enhancement in the value of S rises the temperature and concentration fields. The impact of Prandtl number Pr and Lewis number Le on temperature and concentration fields, respectively, are visualized in Fig. 7. We noted that the increase in Pr and Le result in decreases the thermal and mass diffusivity of naoliquid which declines the temperature and concentration in the Maxwell fluid flow. The temperature field for the effects of heat source/sink δ is illustrated in Fig. 8. The temperature field increases for higher values of heat source and it declines for increasing heat sink parameter. Physically, the heat source provides the additional heat to the liquid which enhances the temperature field and converse behavior is true for heat sink parameter. Moreover, for $\delta < 0$ much heat is absorbed which declines temperature field. The effect of radiation parameter R_d on temperature field is illustrated in Fig. 9. We noted that the increase in values of R_d results in an enhancement in the heat transfer rate. Physically, the increase in R_d rises the ambient temperature of nanofluid and declines the mean absorption coefficient. Hence, the heat transfer rate increases which enhances the temperature field.

Tabular comparisons

Tables 1 and 2 are assessment tables of $-f''(0)$ for different values of β_1 and S for Newtonian case. Table 3 is a comparison of $-\theta'(0)$ in limiting case for various values of Pr. From these tables, we noted that the current outcomes are appropriate which assured the validation of our scheme. Table 4 is also established for the Numerical values of Nusselt and Sherwood numbers for various values of N_t, N_b, R_d and M. These numerical values of Nusselt and Sherwood number are obtained by utilizing the built in MATLAB scheme namely as bvp4c. From these results we conclude that the higher value of both thermophoretic and Brownian forces decline the thermal gradient at the surface of cylinder.

Concluding remarks

A mathematical analysis for unsteady 2D flow of radiative Maxwell nanofluid with heat and mass transport in presence of heat source/sink has been achieved. Homotopy approach (HAM) has been utilized for the solutions of ODEs. The final conclusions of our study are given below:

- The unsteadiness parameter S enhanced both the temperature and concentration distributions.
- Both temperature and concentration fields enhanced for higher values of curvature parameter α.
- An increase in the value of Maxwell parameter β_1 augmented both the temperature and concentration fields.
- Temperature of Maxwell fluid intensified for increasing Brownian motion parameter N_b whereas, conflicted behavior was noted on concentration field.
- The temperature fields declined for higher value of Prandtl number Pr.
- Increase in radiation parameter R_d boost up the temperature profile.

References

Abel MS, Tawade JV, Nandeppanavar MM (2012) MHD flow and heat transfer for upper-convective Maxwell fluid over streching sheet. Meccanica 47:385–393

Ahmed J, Khan M, Ahmad L (2019) Transient thin film flow of nonlinear radiative Maxwell nanofluid over a rotating disk. Phys Lett A 383:1300–1305

Bai Y, Huo L, Zhang Y, Jiang Y (2019) Flow, heat and mass transfer of three-dimensional fractional Maxwell fluid over a bidirectional stretching plate with fractional Fourier's law and fractional Fick's law. Comput Math Appl 78(8):2831–2846

Chamkha AJ, Aly AM, Mansour MA (2010) Similarity solution for unsteady heat and mass transfer from a streching surface

embedded in a porous medium with suction/injection and chemical reaction effects. Chem Eng Commun 197:846–858
Choi SUS (1995) Enhancing thermal conductivity of fluids with nanoparticles. ASME Int Mech Eng 66:99–105
Ellahi R, Zeeshan A, Hussain F, Asadollahi A (2019) Peristaltic blood flow of couple stress fluid suspended with nanoparticles under the influence of chemical reaction and activation energy. Symmetry. https://doi.org/10.3390/sym11020276
Gorla RSR, Sidawi I (1994) Free convection on the verticle stretching surface with suction and blowing. Appl Sci Res 52:247–257
Hamid A, Hashim, Khan M (2018) Impacts of binary chemical reaction with activation energy on unsteady flow of magneto-Williamson nanofluid. J Mol Liq 262:435–442
Haq RU, Aman S (2019) Water functionalized CuO nanoparticles filled in a partially heated trapezoidal cavity with inner heated obstacle: FEM approach. Int J Heat Mass Transf 128:401–417
Hayat T, Rashid M, Alsaedi A, Asghar S (2019) Nonlinear convective flow of Maxwell nanofluid past a stretching cylinder with thermal radiation and chemical reaction. J Br Soc Mech Sci Eng. https://doi.org/10.1007/s40430-019-1576-3
Hsiao KL (2016) Stagnation electrical MHD nanofluid mixed convection with slip boundary on a stretching sheet. Appl Therm Eng 98:850–861
Hsiao KL (2017) Micropolar nanofluid flow with MHD and viscous dissipation effects towards a stretching sheet with multimedia feature. Int J Heat Mass Transf 112:983–990
Hsiao KL (2017a) To promote radiation electrical MHD activation energy thermal extrusion manufacturing system efficiency by using Carreau-Nanofluid with parameters control method. Energy 130:486–499
Hsiao KL (2017b) Combined electrical MHD heat transfer thermal extrusion system using Maxwell fluid with radiative and viscous dissipation effects. Appl Therm Eng 112:1281–1288
Irfan M, Khan M, Khan WA (2017) Numerical analysis of unsteady 3D flow of Carreau nanofluid with variable thermal conductivity and heat source/sink. Results Phys 7:3315–3324
Irfan M, Khan WA, Khan M, Gulzar MM (2019) Influence of Arrhenius activation energy in chemically reactive radiative flow of 3D Carreau nanofluid with nonlinear mixed convection. J Phys Chem Solids 125:141–152
Irfan M, Khan M, Khan WA (2019) Impact of homogeneous–heterogeneous reactions and non-Fourier heat flux theory in Oldroyd-B fluid with variable conductivity. J Br Soc Mech Sci Eng. https://doi.org/10.1007/s12043-018-1690-2
Khan MN, Nadeem S (2019) Theoretical treatment of bio-convective Maxwell nanofluid over an exponentially stretching sheet. Can J Phys. https://doi.org/10.1139/cjp-2019-0380
Khan WA, Pop I (2010) Boundary-layer flow of a nanofluid past a stretching sheet. Int J Heat Mass Transf 53:2477–2483
Khan MI, Kumar A, Hayat T, Waqas M, Singh R (2019) Entropy generation in flow of Carreau nanofluid. J Mol Liq 278:677–687
Khan M, Irfan M, Khan WA (2019) Heat transfer enhancement for Maxwell nanofluid flow subject to convective heat transport. Pramana J Phys. https://doi.org/10.1007/s12043-018-1690-2
Mahanthesh B, Joseph TV (2019) Dynamics of magneto-nano third-grade fluid with Brownian Motion and thermophoresis effects in the pressure type die. J Nanofluids 136:288–297
Malik R, Khan M (2018) Numerical study of homogeneous-heterogeneous reactions in Sisko fluid flow past a stretching cylinder. Results Phys 8:64–70
Megahed AM (2013) Variable fluid properties and variable heat flux effects on the flow and heat transfer in non-Newtonian Maxwell fluid over an unsteady streching sheet with slip velocity. Chin Phys B. https://doi.org/10.1088/1674-1056/22/9/094701
Moshkin NP, Pukhnachev VV, Bozhkov YD (2019) On the unsteady, stagnation point flow of a Maxwell fluid in 2D. Int J Non-Linear Mech 116:32–38
Sharidan S, Mahmood M, Pop I (2006) Similarity solutions for the unsteady boundary layer flow and heat transfer due to a streching sheet. Int J Appl Mech Eng 11:647–654
Turkyilmazoglu M (2011) Convergence of the homotopy perturbation method. Int J Nonlinear Sci Numer Simul 12:1–8
Turkyilmazoglu M (2012) An effective approach for approximate analytical solutions of the damped Duffing equation. Phys Scr 86:1
Turkyilmazoglu M (2018) Convergence accelerating in the homotopy analysis method: a new approach. Adv Appl Math Mech 10:925–947
Turkyilmazoglu M (2019a) Free and circular jets cooled by single phase nanofluids. Eur J Mech B Fluids 76:1–6
Turkyilmazoglu M (2019b) Fully developed slip flow in a concentric annuli via single and dual phase nanofluids models. Comput Methods Progr Biol 179:104997
Turkyilmazoglu M (2020) Single phase nanofluids in fluid mechanics and their hydrodynamic linear stability analysis. Comput Methods Progr Biol 179:105171
Wang CY (1989) Free convection on a vertical stretching surface. ZAMM 69:418–420
Waqas M, Khan MI, Hayat T, Alsaedi A (2017) Stratified flow of an Oldroyd-B nanofluid with heat generation. Results Phys 7:2489–2496
Xu HJ, Xing ZB, Wang FQ, Cheng ZM (2019) Review on heat conduction, heat convection, thermal radiation and phase change heat transfer of nanofluids in porous media: fundamentals and applications. Chem Eng Sci 195:462–483